Biochimie 95 (2013) 1784–1794

Contents lists available at SciVerse ScienceDirect

Biochimie

journal homepage: www.elsevier.com/locate/biochi

Research paper

Two peptides, TsAP-1 and TsAP-2, from the venom of the Brazilian yellow scorpion, *Tityus serrulatus*: Evaluation of their antimicrobial and anticancer activities

Xiaoxiao Guo [1], Chengbang Ma [1], Qiang Du, Ran Wei, Lei Wang*, Mei Zhou*, Tianbao Chen, Chris Shaw

Molecular Therapeutics Research, School of Pharmacy, Queen's University Belfast, Medical Biology Centre, Belfast BT9 7BL, Northern Ireland, UK

ARTICLE INFO

Article history:
Received 28 March 2013
Accepted 5 June 2013
Available online 14 June 2013

Keywords:
Scorpion
Molecular cloning
Antimicrobial
Peptide

ABSTRACT

Here we report two novel 17-mer amidated linear peptides (TsAP-1 and TsAP-2) whose structures were deduced from cDNAs cloned from a venom-derived cDNA library of the Brazilian yellow scorpion, *Tityus serrulatus*. Both mature peptides were structurally-characterised following their location in chromatographic fractions of venom and synthetic replicates of each were subjected to a range of biological assays. The peptides were each active against model test micro-organisms but with different potencies. TsAP-1 was of low potency against all three test organisms (MICs 120–160 μM), whereas TsAP-2 was of high potency against the Gram-positive bacterium, *Staphylococcus aureus* (MIC 5 μM) and the yeast, *Candida albicans* (10 μM). Haemolytic activity of TsAP-1 was low (4% at 160 μM) and in contrast, that of TsAP-2 was considerably higher (18% at 20 μM). Substitution of four neutral amino acid residues with Lys residues in each peptide had dramatic effects on their antimicrobial potencies and haemolytic activities, particularly those of TsAP-1. The MICs of the enhanced cationic analogue (TsAP-S1) were 2.5 μM for *S. aureus*/*C. albicans* and 5 μM for *E. coli* but with an associated large increase in haemolytic activity (30% at 5 μM). The same Lys residue substitutions in TsAP-2 produced a dramatic effect on its MIC for *E. coli* lowering this from >320 μM to 5 μM. TsAP-1 was ineffective against three of the five human cancer cell lines tested while TsAP-2 inhibited the growth of all five. Lys residue substitution of both peptides enhanced their potency against all five cell lines with TsAp-S2 being the most potent with IC_{50} values ranging between 0.83 and 2.0 μM. TsAP-1 and TsAP-2 are novel scorpion venom peptides with broad spectrum antimicrobial and anticancer cell activities the potencies of which can be significantly enhanced by increasing their cationicity.

© 2013 Elsevier Masson SAS. All rights reserved.

1. Introduction

Scorpion venom is one of the richest natural sources of peptide toxins. A large number of these are toxic to both vertebrates and invertebrates through their highly-specific targeted interactions with the ion-channel membrane proteins of both excitable and non-excitable cells. Through efficient use of this toxic molecular arsenal, scorpions can employ such for many purposes including prey capture, defence and competitor deference [1–4]. Although this complex cocktail of biologically-active molecules appears to have evolved primarily for subduing prey, it also plays a highly-effective role in chemical defence as any human who has ever touched a scorpion, either intentionally or otherwise, will testify [1–4].

The majority of the peptide neurotoxins present in scorpion venoms exert their devastating effects by targeting a group of the most fundamental of molecular complexes that are essential cell membrane components in all forms of life - the ion channels [5–8]. The ion channel-interacting toxins target their cognate ion channels with affinities and selectivities that are among the highest recorded between biomolecules [5–8]. As ion channels are the predominant essential functional components in excitable tissues such as muscles and nerves, their disruption can rapidly lead to respiratory and circulatory damage that can cause death. Leaving aside the fact that scorpion envenomation can cause significant human morbidity and even mortality, these peptides are useful ion channel characterisation and neurobiological study tools [5–8].

* Corresponding authors. Tel.: +44 (0) 2890972200; fax: +44 (0) 2890247794.
E-mail addresses: l.wang@qub.ac.uk (L. Wang), m.zhou@qub.ac.uk (M. Zhou).
[1] These authors contributed equally to this work.

0300-9084/$ – see front matter © 2013 Elsevier Masson SAS. All rights reserved.
http://dx.doi.org/10.1016/j.biochi.2013.06.003

Biochemical studies on scorpion venoms have a long history but over the past two decades, coincident with the vast improvements in protein/peptide isolation and characterisation technology [9], structures of scorpion venom neurotoxins have been elucidated in significant numbers [10]. Most scorpion venom neurotoxins consist of 23–78 amino acid residues stabilised by 3–4 disulphide bridges and these specifically target mostly Na^+ and K^+ ion channels, which are essential elements in the control of many physiological processes in many life forms [7,8].

Of more recent discovery in scorpion venoms, are the low molecular mass (<3 kDa) peptides, the majority of which are devoid of disulphide bridges [10,11]. Although unstudied for a considerable period of time, mass analyses of many different scorpion venoms have revealed that this broad group of peptides accounts for more than one third of all the peptides present [12]. This group of peptides are highly-diverse in both their primary structures and their bioactivities rendering them a potentially-interesting group on which to focus research efforts [1,10,11].

Here we report the structures and biosynthetic precursor organisations of two non disulphide-bridged antimicrobial and anticancer cell peptides from the venom of the Brazilian yellow scorpion, *Tityus serrulatus*. Named TsAP-1 and -2, they exhibit high degrees of primary structural similarity with the amphibian skin antimicrobial peptides, phylloseptins and the recently described medusins, respectively [13,14]. In addition, the biological effects of synthetic analogues of each natural peptide, engineered for enhanced cationicity/amphipathicity, were assessed.

2. Materials and methods

2.1. Acquisition of Tityus serrulatus venom

Twenty milligrams of lyophilised *Tityus serrulatus* venom were obtained from Latoxan, Valence, France. The scorpions were collected in the field and identified by experts before relocation to the company in France. Venom was collected by trained individuals using mild electrical stimulation (15 V) consistent with obtaining sufficient material but also with causing a negligible degree of damage to the animals. Venom samples were obtained by this procedure at regular intervals for considerable periods of time (Latoxan, personal communication).

2.2. "Shotgun" cloning of venom peptide precursor-encoding cDNAs

Five milligrams of lyophilised *Tityus serrulatus* venom (Latoxan, France) were dissolved in 1 ml of cell lysis/binding buffer (Dynal Ltd, UK). Polyadenylated mRNA was isolated by using magnetised oligo-dT beads as described by the manufacturer (Dynal, UK) and reverse transcribed. This cDNA was subjected to 3′-RACE procedures to obtain full-length venom peptide precursor-encoding nucleic acid sequence data using a SMART-RACE kit (Clontech, UK) essentially as described by the manufacturer. Briefly, the 3′-RACE reactions employed a nested universal primer (NUP), supplied with the kit, and a sense primer (S1; 5′-CATGCAATTAAAA-CATCTCATTACT-3′) that was designed to a highly-conserved nucleic acid sequence occurring within the signal peptide-encoding region of previously-cloned antimicrobial peptide cDNAs from the closely-related scorpion species, *Tityus costatus* (Genbank accession nos. AY740686.1 – AY740688.1). The PCR cycling procedure was as follows: Initial denaturation step: 60 s at 94 °C; 35 cycles: denaturation 30 s at 94 °C, primer annealing for 30 s at 55 °C; extension for 180 s at 72 °C. Resultant PCR products were gel-purified, cloned using a pGEM-T vector system (Promega Corporation) and sequenced using an ABI 3100 automated DNA sequencer.

2.3. Identification and structural analysis of putative cDNA-encoded antimicrobial peptides

A second 5 mg sample of lyophilised *Tityus serrulatus* venom was dissolved in 0.5 ml of 0.05/99.95 (v/v) trifluoroacetic acid (TFA)/water and clarified by centrifugation. The supernatant was decanted and directly subjected to reverse-phase HPLC fractionation using a Cecil CE4200 Adept (Cambridge, UK) gradient reverse phase HPLC system fitted with an analytical column (Phenomenex C-5, 0.46 cm × 25 cm). The linear elution gradient employed was formed from 0.05/99.95 (v/v) TFA/water to 0.05/19.95/80.0 (v/v/v) TFA/water/acetonitrile in 240 min at a flow rate of 1 ml/min. The chromatographic system employed was interfaced with an LCQ Fleet™ electrospray ion-trap mass spectrometer (Thermo Fisher, San Jose, CA, USA) with the effluent flow from the HPLC column being flow split with 95% directed to a fraction collector and 5% directed into the electrospray source of the mass spectrometer. By means of data-dependent acquisition, doubly-charged peptide ions detected in the mass spectrometer were automatically subjected to MS/MS fragmentation.

2.4. Prediction of putative peptide secondary structures and physicochemical properties

Putative peptide secondary structures were predicted using PHD secondary structure prediction method software (Pôle Bioinformatique Lyonnais). Additional physicochemical properties, including molecular mass and net charge at neutral pH, were determined using the Innovagen peptide property calculator, while α-helical wheel plots were constructed by use of the helical wheel projection modeller present on the Helical wheel Applet (http://lectures.molgen.mpg.de/Individual/HelicalWheel/). The relative hydrophobic moments of each peptide were determined using the HydroMCalc (http://www.bbcm.univ.trieste.it/∼tossi/HydroCalc/HydroMCalc.html) method software (Kyte et al., 1982), which evaluated the amphipathicity of each peptide.

2.5. Peptide synthesis and purification

The two natural peptides and their enhanced cationicity/amphipathicity analogues, were synthesised by solid phase methodology using Rink amide resin and standard Fmoc chemistry, by means of an automated PS3 peptide synthesiser (Protein Technologies, USA), followed by deprotection and cleavage from the resin. All synthetic peptides were purified by reverse phase HPLC and both their authenticity of structure and degree of purity were confirmed by use of electrospray mass spectrometry.

2.6. Antimicrobial assays

The antimicrobial activity of each synthetic peptide was assessed by means of determining minimal inhibitory concentrations (MICs) against model strains of Gram-positive bacteria, *Staphylococcus aureus* (NCTC 10788), Gram-negative bacteria, *E. coli* (NCTC 10418) and yeast, *Candida albicans* (NCPF 1467), respectively. The model micro-organisms were initially incubated in Mueller-Hinton Broth (MHB) for 16–20 h. Upon achieving their respective logarithmic growth phases, as measured by the optical density (OD) of media at 550 nm, the cultures were diluted to 1×10^6 colony-forming units (cfu)/ml for the bacteria and to 5×10^5 cfu/ml for the yeast. Samples of these were then added to 96-well microtitre plates and mixed with the tested peptides at various concentrations. After 24 h incubation, the OD of each well was measured at 550 nm using a Synergy HT plate reader (BioTek, USA), and the data were analysed using Graph Pad Prism 5 software. The MIC was

defined as the minimum concentration of peptide with an OD the same as the negative control. After this, 10 μl of the medium from each well was inoculated onto a Mueller Hinton agar (MHA) plate and incubated for 24 h for measurement of minimum bactericidal concentrations (MBCs) which was defined as the concentration of peptide from which no colonies could be grown.

2.7. Haemolysis assay

The haemolytic activity of each peptide was measured by incubating a range of concentrations of each synthetic peptide with a 4% suspension of horse erythrocytes that had been previously prepared by repeated washings with sterile PBS, centrifugations and resuspensions. After incubation for 120 min, the suspensions were centrifuged at 900×*g* for 5 min to pellet but not disrupt the cells. Optical density (OD) measurements of supernatants at 550 nm, were recorded using a Synergy HT plate reader. The incubation of erythrocytes with 1% (v/v) Triton X-100 was designated as a positive control (100% haemolysis) and with PBS as a negative control (0% haemolysis).

2.8. Culture and maintenance of human cancer cell lines

The human squamous carcinoma cell line, NCI–H157, the human lung adenocarcinoma cell line, NCI–H838 and the human androgen-independent prostate adenocarcinoma cell line, PC-3, were cultured using RPMI-1640 culture medium (Invitrogen). Before culturing the cells, this medium was supplemented with 10% (v/v) foetal bovine serum (FBS) (Sigma) and 0.1% (w/v) gentamicin (Sigma) and the cells were seeded into 150 cm^2 culture flasks (Nunc, UK). The human breast carcinoma cell line, MCF-7, and the U251 human glioblastoma cell line, were cultured using a Dulbecco's Modified Eagle's Medium (DMEM) (Sigma), which was supplemented with 10% FBS and 0.1% gentamicin. The cells were seeded into 150 cm^2 culture flasks.

2.9. Assessment of anti-proliferative effects of TsAPs on human cancer cells using the MTT cell viability assay

Yellow-coloured MTT (3-(4,5-dimethylthiazol-2-yl)-2,5-diphenyltetrazolium bromide) is reduced by the mitochondria of living cells to form a purple-coloured (formazan) crystalline derivative. These crystals can be solubilised by the addition of dimethyl sulphoxide (DMSO) and their concentration determined spectrophotometrically, as detailed below.

The protocol employed has been described in detail previously [15]. Briefly, each cell line was seeded at a density of 5 × 10^3 cells per well on 96-well plates. After this, cells were treated with various concentrations of peptides or with serum-free medium alone and were incubated for 24 h. Following this,

A)

```
       M  Q  I   K  H  L  I   T  L  F   F  L  V   L  I  V  A
  1   ATGCAAATAA AACATCTCAT TACTCTCTTC TTTCTCGTCT TGATCGTTGC
      TACGTTTATT TTGTAGAGTA ATGAGAGAAG AAAGAGCAGA ACTAGCAACG
        D  Q  C   S  A  F   L  S  L  I   P  S  L   V  G  G
 51   TGATCAGTGC TCGGCTTTCC TTTCTTTAAT TCCGTCACTG GTAGGTGGTT
      ACTAGTCACG AGCCGAAAGG AAAGAAATTA AGGCAGTGAC CATCCACCAA
      S  I  S  A   F  K  G   R  R  K   R  E  I  S   A  Q  I
101   CGATTTCTGC ATTCAAGGGC AGAAGGAAAA GAGAGATCTC CGCGCAGATT
      GCTAAAGACG TAAGTTCCCG TCTTCCTTTT CTCTCTAGAG GCGCGTCTAA
        E  Q  Y   K  D  L  Q   K  R  E   A  E  L   E  E  L  L
151   GAGCAGTACA AAGATCTTCA GAAGCGCGAA GCCGAGTTAG AGGAACTTTT
      CTCGTCATGT TTCTAGAAGT CTTCGCGCTT CGGCTCAATC TCCTTGAAAA
        D  R  L   P  M  Y   *
201   AGATAGATTG CCGATGTATT AATTTCATTA AATTATATTG CCATTTATAA
      TCTATCTAAC GGCTACATAA TTAAAGTAAT TTAATATAAC GGTAAATATT
251   TAATAATAAG ACTGCTGTTT CGACTTTAAT TCCTATACTT TTATTTCTAA
      ATTATTATTC TGACGACAAA GCTGAAATTA AGGATATGAA AATAAAGATT
301   ATAACAAGAA AAAAAAAAAA AAAAAAAAAA AAAAAAA
      TATTGTTCTT TTTTTTTTTT TTTTTTTTTT TTTTTTT
```

B)

```
       M  Q  I   K  H  L  I   T  I  F   F  L  V   L  I  V  A
  1   ATGCAAATAA AACATCTCAT TACTATTTTC TTCCTCGTCT TGATCGTTGC
      TACGTTTATT TTGTAGAGTA ATGATAAAAG AAGGAGCAGA ACTAGCAACG
        D  H  C   H  A  F   L  G  M  I   P  G  L   I  G  G
 51   CGATCATTGC CACGCTTTTC TTGGTATGAT CCCTGGATTG ATAGGTGGTT
      GCTAGTAACG GTGCGAAAAG AACCATACTA GGGACCTAAC TATCCACCAA
      L  I  S  A   F  K  G   R  R  K   R  E  I  T   S  Q  I
101   TGATTTCTGC ATTCAAGGGC AGAAGGAAGC GAGAAATTAC TTCACAAATC
      ACTAAAGACG TAAGTTCCCG TCTTCCTTCG CTCTTTAATG AAGTGTTTAG
        E  Q  Y   R  N  L  Q   K  R  E   A  E  L   E  N  L  L
151   GAACAATACA GAAATCTCCA GAAGCGTGAA GCGGAGTTAG AAAACCTTTT
      CTTGTTATGT CTTTAGAGGT CTTCGCACTT CGCCTCAATC TTTTGGAAAA
        A  N  L   P  V  Y   *
201   GGCTAATTTG CCGGTTTATT AATTACATTA GAGTATTGAA ATATATAATA
      CCGATTAAAC GGCCAAATAA TTAATGTAAT CTCATAACTT TATATATTAT
251   ATAGGACTGC TGCCTCAAAA TTAACTCCAA TATTTTTATT TTTAAACAAT
      TATCCTGACG ACGGAGTTTT AATTGAGGTT ATAAAAATAA AAATTTGTTA
301   AAAAAATTAC AAAAAAAAAA AAAAAAAAAA AAAAAAAA
      TTTTTTAATG TTTTTTTTTT TTTTTTTTTT TTTTTTTT
```

Fig. 1. Nucleotide and translated open-reading frame amino acid sequences of cloned cDNAs encoding the biosynthetic precursors of TsAP-1 (A) and TsAP-2 (B). Putative signal peptide sequences are double-underlined, mature antimicrobial peptide sequences are single-underlined and stop codons are indicated by asterisks. Note conserved basic amino acid propeptide convertase cleavage sites (-RRKR-) following the mature peptide sequences and the strategically-placed glycyl (G) residues that act as amide donors for the C-terminal lysyl (K) residues in both mature peptides.

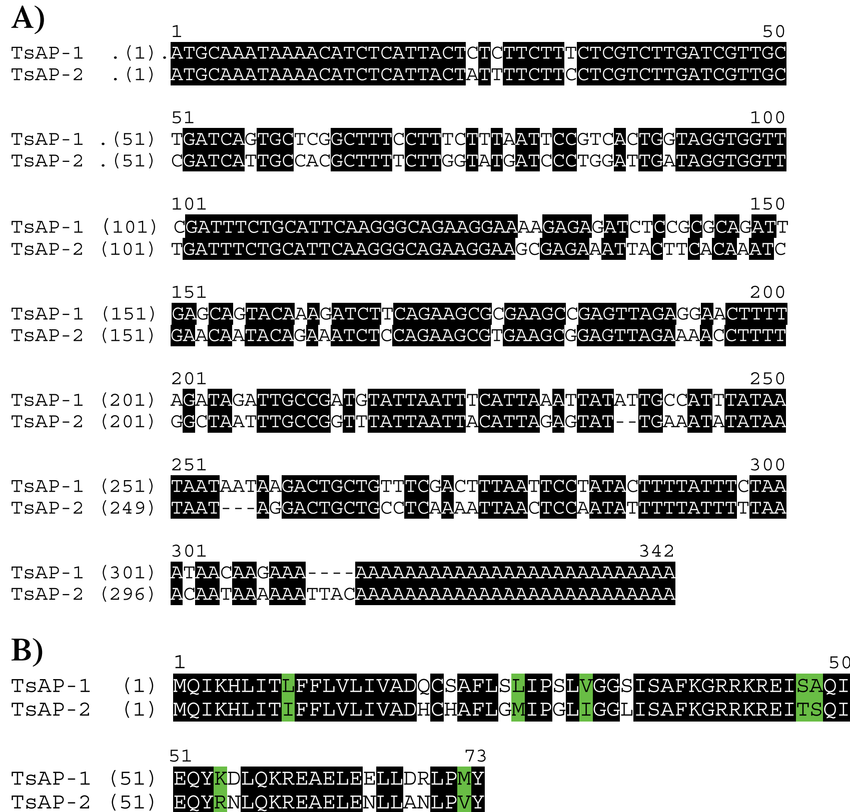

Fig. 2. Alignments of nucleotide sequences of cloned cDNAs encoding the biosynthetic precursors of TsAP-1 and -2 (A) and open-reading frame amino acid sequences (B). Conserved nucleotides and amino acid residues are shaded in black. Within open-reading frames, conservative amino acid substitutions are shaded grey and non-conservative substitutions are unshaded.

10 μl of a 5 mg/ml MTT solution was added to each well and the plates incubated again for 4 h. The growth medium was later removed using a 1 ml syringe fitted with a needle and 100 μl of DMSO were added to each well and mixed vigorously to dissolve the formazan crystals that had developed. The absorbance was measured using an ELx808™ Absorbance Microplate Reader (BioTek, USA) at 550 nm and the statistical analyses were performed using Student's *t*-test through GraphPad prism software for Windows. The results were considered to be statistically significant if the p value was <0.05.

3. Results

3.1. "Shotgun" molecular cloning of putative antimicrobial peptide precursor-encoding cDNAs

Using the molecular cloning strategy described, two different full-length cDNAs were consistently cloned from the *Tityus serrulatus* venom-derived cDNA library, each encoding a single copy of a putative antimicrobial peptide (Fig. 1A and B). The nucleic acid sequences of each novel open-reading frame were

1. ***Tityus serrulatus*** antimicrobial peptide 1	**FLSLIPSLVGGSISAFK**
2. ***Tityus costatus*** antimicrobial peptide clone 4	**--GM--G-I--L-----**
3. ***Tityus costatus*** antimicrobial peptide clone 6	**-F------I--LV--I-**
4. ***Lychas mucronatus*** antimicrobial peptide 36.21	**LFG-----I--LV----**
5. ***Mesobuthus martensii*** Kb1* peptide	**--F----AIS-L-----**
6. ***Mesobuthis eupeus* caerin** antibacterial peptide	**--F----AIS-L-----**
7. ***Phyllomedusa hypochondrialis*** phylloseptin-10	**----L----S-AV-LV-KL**
8. ***Phyllomedusa hypochondrialis*** phylloseptin-11	**----L----S-AV-LV-IL**

Database Accession nos.: 1. HF677516. 2. Q5G8B5. 3. Q5G8B3. 4. B9UIY3.1. 5. AAK61826.1. 6. AGC92780.1.

Fig. 3. Summary of the BLAST results from the NCBI database using TsAP-1 (#1) as the query sequence. The first five hits (#s 2–6) are with antimicrobial peptides from the venoms of other scorpions. There was also a high degree of N-terminal primary structural identity with antimicrobial peptides (#s 7 and 8) - the phylloseptins- from the skin of a phyllomedusine frog, (*Phyllomedusa hypochondrialis*). Accession numbers for each peptide are shown in the footnote.

1. *Tityus serrulatus* antimicrobial peptide 2	**FLGMIPGLIGGLISAFK**
2. *Tityus costatus* antimicrobial peptide clone 4	**-----------------**
3. *Lychas mucronatus* antimicrobial peptide 36.21	**LF-L--S-----V----**
4. *Lychas mucronatus* antimicrobial peptide NDBP 13	**-- -S----------**
5. *Pachymedusa dacnicolor* phyllin/medusin-PD	**L-----LA-SAIS-LS-L**

Database accession nos.: 1. HF677517. 2. Q5G8B5.1. 3. B9UIY3.1. 4. D9U2B8.1. 5. CCI79381.1.

Fig. 4. Summary of the BLAST results from the NCBI database using TsAP-2 (#1) as the query sequence. The first three hits (#s 2–4) are with antimicrobial peptides from the venoms of other scorpions. There was also a high degree of N-terminal primary structural identity with an antimicrobial peptide (# 5) – phyllin/medusin-PD- from the skin of a phyllomedusine frog, (*Pachymedusa dacnicolor*). Accession numbers for each peptide are shown in the footnote.

confirmed in at least 15 clones. No other peptide precursor-encoding clones were identified using the cloning strategy described. Alignments of full length nucleic acid sequences (Fig. 2A) and the open-reading frame amino acid sequences (Fig. 2B) of these peptide precursor-encoding cDNAs, showed that they were highly-homologous in both respects. Their respective putative signal peptides consisted of 22 predominantly-hydrophobic amino acid residues that were

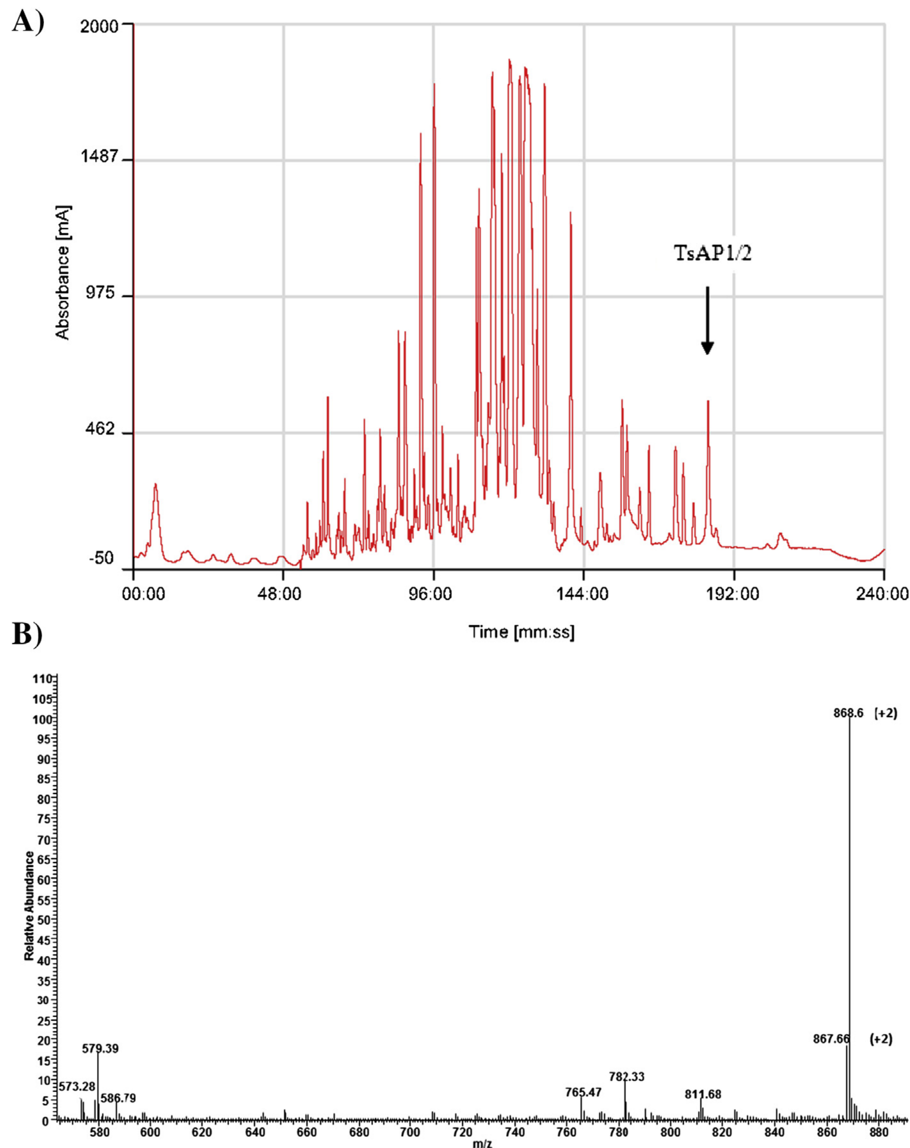

Fig. 5. Reverse phase HPLC trace of lyophilised *Tityus serrulatus* venom with the retention time/elution position of TsAP-1/2 indicated with an arrow. The linear elution gradient employed was formed from 0.05/99.95 (v/v) TFA/water to 0.05/19.95/80.0 (v/v/v) TFA/water/acetonitrile in 240 min at a flow rate of 1 ml/min (A). Electrospray mass spectrum of reverse phase HPLC fraction containing TsAP-1/2 showing doubly-charged ions $(M + 2H)^{2+}$ at m/z 867.66 and m/z 868.60 (B) corresponding to computed parent molecular masses of 1733.32 Da (TsAP-2) and 1735.20 Da (TsAP-1).

highly-conserved exhibiting only 3 variant amino acid positions. The cleavage of signal peptides appeared to occur between Ala[22] and the N-terminal Phe residues of the antimicrobial peptides that each consisted of 17 amino acid residues with 5 variant amino acid positions. Each peptide was flanked C-terminally by a Gly residue amide donor and a sequence of 4 basic amino acid residues (-Arg-Arg-Lys-Arg-) that contained the propeptide convertase cleavage motif. The peptides were named *Tityus serrulatus* antimicrobial peptide 1(TsAP-1) and −2 (TsAP-2), respectively. A BLAST search in the EMBL Nucleotide Sequence Database revealed that both peptides exhibited high degrees of structural similarity to other reported antimicrobial peptides from other scorpions. In addition, their biosynthetic precursor sequences, containing 73–74 amino acid residues, also exhibited striking primary structural similarities in signal peptide and other domains outside of those encoding the mature antimicrobial peptides, implying that these constitute a family of such peptides from scorpion venom. Interestingly, both peptides displayed high degrees of primary structural similarities with phylloseptins (TsAP-1) and medusins (TsAP-2) that are both families of antimicrobial peptides from the skin secretions of phyllomedusine frogs [13,14] (Figs. 3 and 4). The nucleotide sequences of the precursor-encoding cDNAs of both peptides have been deposited in the EMBL Nucleotide Sequence Database under the accession codes HF677516 (TsAP-1) and HF677517 (TsAP-2).

3.2. Isolation and structural characterisation of the TsAPs from reverse phase HPLC fractions of venom

Following deduction of the primary structures and molecular masses of the two novel TsAP peptides from respective cloned cDNAs, both mature peptides were located in the same reverse phase HPLC fraction (#180), following fractionation of *Tityus serrulatus* venom (Fig. 5A) and identified by molecular mass fingerprints in the same HPLC fraction (Fig. 5B). Subsequent electrospray ion-trap MS/MS fragmentation of the doubly-charged ions arising from both mature peptides present in this fraction, confirmed their respective primary structures (Table 1 and Fig. 6). Interestingly, a data-dependent LC/MS/MS analysis of venom, while resolving major ions corresponding to both mature TsAPs, also resolved major ions of peptides corresponding to residues 49–70 of each respective precursor protein. These were tentatively named QL-22 after N- and C-terminal residues and number of residues. These data indicated N-terminal cleavage sites between to A-Q and S-Q within TsAP-1 and TsAP-2 precursors, respectively. The −KR− sites within each peptide did not thus appear to be a major site of propeptide convertase cleavage. The putative activity of these peptides was not addressed in this study.

3.3. Peptide synthesis

TsAP-1 and TsAP-2 were successfully synthesised by the solid-phase Fmoc method using a PS3™ automated peptide synthesiser (Protein Technologies, Tucson, AZ, USA). In addition, an analogue of each peptide, named TsAP-S1 and TsAP-S2, respectively, were also successfully synthesised. These analogues were specifically designed to enhance the cationicity of each natural peptide by Lys residue substitution of Ser^{7}, Gly^{10}, Gly^{1} and Ser^{14} in TsAP-1 and Gly^{7}, Gly^{10}, Gly^{11} and Ser^{14} in TsAP-2. Substitution of Gly residues would also serve to increase the helicity of the natural peptides as this residue is a classical helix breaker. All synthetic peptides were purified by reverse phase HPLC to >95% purity and their structures were confirmed by MS/MS fragmentation sequencing.

Table 1
MS/MS datasets derived from fragmentation of doubly-charged parent ions consistent in molecular mass with (A) TsAP-1 and (B) TsAP-2. Singly- and doubly-charged *b*-ion and *y*-ion fragment series arising from the putative primary structures were predicted using the MS-Product programme available through Protein Prospector online. Fragment ions detected by the ESI-MS/MS software are indicated in bold type-face and are underlined.

#1	b(1+)	b(2+)	Seq.	y(1+)	y(2+)	#2
(A)						
1	148.08	74.54	F			17
2	**261.16**	131.08	L	1587.95	794.48	16
3	**348.19**	174.60	S	**1474.86**	**737.94**	15
4	**461.28**	231.14	L	**1387.83**	**694.42**	14
5	**574.36**	287.68	I	**1274.75**	**637.88**	13
6	671.41	336.21	P	**1161.66**	**581.34**	12
7	758.44	379.73	S	**1064.61**	532.81	11
8	**871.53**	436.27	L	977.58	**489.29**	10
9	**970.60**	**485.80**	V	**864.49**	**432.75**	9
10	**1027.62**	**514.31**	G	**765.43**	383.22	8
11	**1084.64**	542.82	G	**708.40**	354.71	7
12	**1171.67**	**586.34**	S	**651.38**	326.20	6
13	**1284.76**	**642.88**	I	**564.35**	282.68	5
14	**1371.79**	**686.40**	S	451.27	226.14	4
15	**1442.83**	**721.92**	A	**364.23**	182.62	3
16	**1589.89**	**795.45**	F	**293.20**	147.10	2
17			K-Amidated	146.13	73.57	1
(B)						
1	148.08	74.54	F			17
2	**261.16**	131.08	L	1585.95	**793.48**	16
3	**318.18**	159.59	G	**1472.87**	**736.94**	15
4	**449.22**	225.11	M	**1415.84**	708.43	14
5	**562.31**	281.66	I	**1284.80**	**642.91**	13
6	**659.36**	**330.18**	P	**1171.72**	**586.36**	12
7	**716.38**	358.69	G	**1074.67**	537.84	11
8	**829.46**	**415.24**	L	1017.65	509.33	10
9	**942.55**	471.78	I	**904.56**	**452.78**	9
10	**999.57**	**500.29**	G	**791.48**	396.24	8
11	**1056.59**	528.80	G	**734.46**	367.73	7
12	**1169.68**	585.34	L	**677.43**	339.22	6
13	**1282.76**	**641.88**	I	**564.35**	282.68	5
14	**1369.79**	685.40	S	**451.27**	226.14	4
15	**1440.83**	**720.92**	A	**364.23**	182.62	3
16	**1587.90**	**794.45**	F	**293.20**	147.10	2
17			K-Amidated	146.13	73.57	1

3.4. Secondary structure prediction and physiochemical properties of TsAPs and their analogues

Table 2 summarises the results of determinations of these parameters. Both TsAP-1 and -2 at pH 7, had net positive charges of +2 as a result and combination of their free N-terminal amino groups, the side chains of their conserved Lys^{17} residues, their common amidated C-terminals and their lack of acidic amino acid residues. Despite their common cationicity, the two peptides differed significantly in their predicted helical content with TsAP-1 containing 58.82% and TsAP-2, 76.47%. Both peptides also differed in their hydrophobic moments. In contrast, while the net positive charge of each synthetic analogue increased to +6 as expected through incorporation of an additional 4 Lys residues, unexpectedly, these modifications resulted in enhancing the helical content of both natural peptides to 88.24% and providing both with virtually identical and enhanced hydrophobic moments of 0.75 μH and 0.73 μH, respectively. These data indicate that the two synthetic analogues possessed similar α-helical amphipathic structures. Helical wheel plots of all four peptides are shown in Fig. 7. From these, it can be clearly seen that the sites of Lys substitutions on each natural peptide, although apparently spaced along the peptide chain, have side-chains that are orientated in the same planar face of the peptide. Note also that the hydrophobic residue side chains occupy the opposite planar space. Thus the structural modifications in TsAP-S1 and TsAP-S2 have produced classical optimised amphipathic peptides.

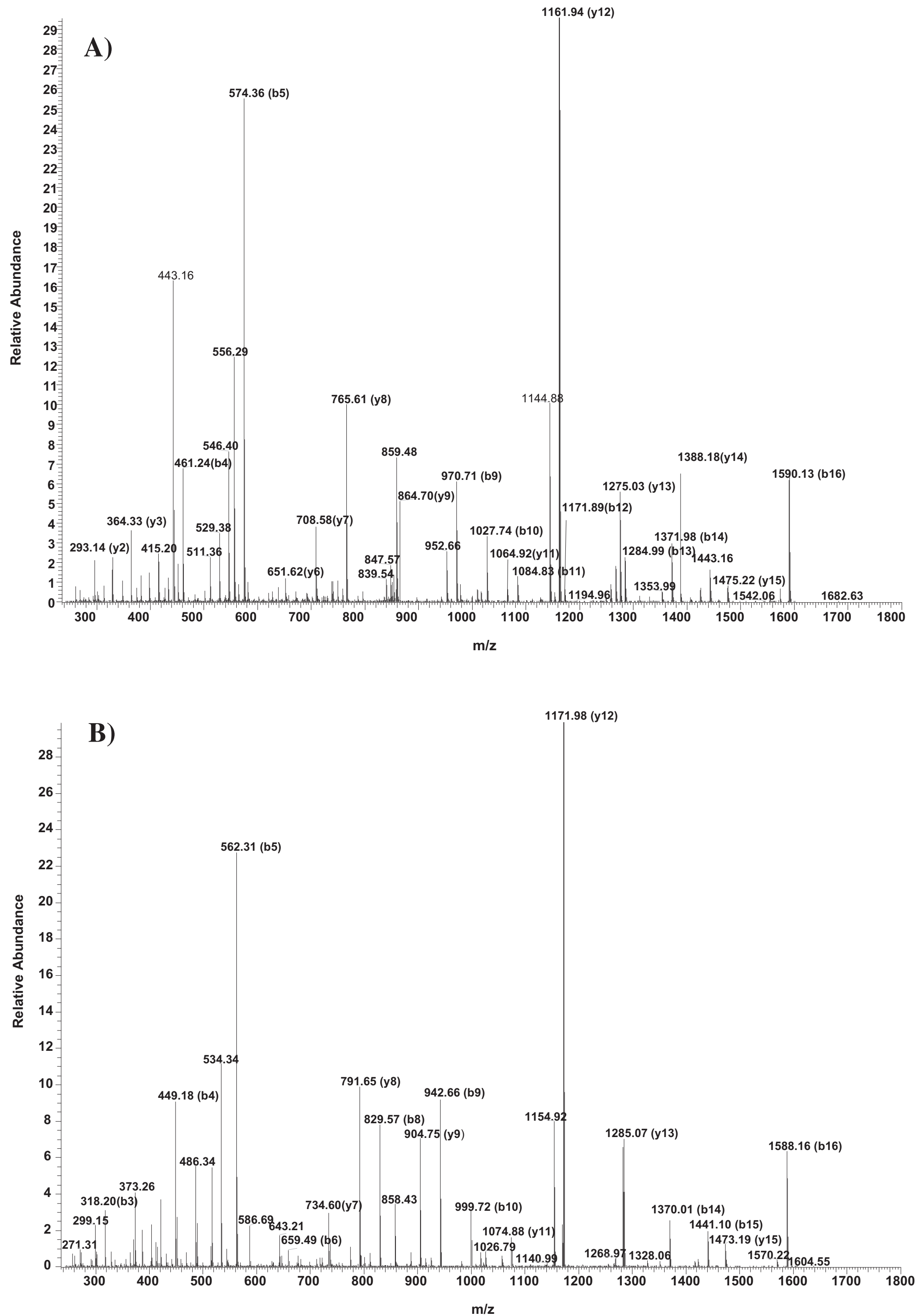

Fig. 6. ESI MS/MS fragmentation spectra of (A) TsAP-1 and (B) TsAP-2. Respective *b*-ions and *y*-ions identified visually are annotated in each spectrum.

3.5. Antimicrobial effects of TsAPs

The data obtained from both MIC and MBC assays of the natural TsAPs and their analogues are summarised in Table 3. TsAP-1 was of the lowest potency in both assays against all three model test organisms. TsAP-2, in contrast, was potent against the Gram-positive bacterium, *S. aureus*, and the yeast, *C. albicans*, in both assays, at concentrations around 5–10 μM. However, this peptide was virtually ineffective against the Gram-negative bacterium, *E. coli*. The cationicity-enhanced analogues of both peptides, however, displayed impressive increases in both antimicrobial potency and spectrum of activity in both assays. The most spectacular change was observed between the MICs of TsAP-2 and TsAP-S2 against *E. coli* which changed from >320 μM to 5 μM.

Table 2
Secondary structure predictions and some physiochemical properties of TsAPs and their enhanced cationicity analogues described in this study. Net charges were calculated at pH 7. Random coils are represented by c in normal typeface and helices by h in bold typeface.

Peptides	Secondary structure	α-helix (%)	Hydrophobic moment (μH)	Net charge
(A)				
TsAP-1	FLSLIPSLVGGSISAFK cccc**hhhhh**c**hhhhh**cc	58.82	0.43	+2
TsAP-2	FLGMIPGLIGGLISAFK ccc**hhhhhhhhhhhhh**c	76.47	0.51	+2
TsAP-S1	FLSLIPKLVKKIIKAFK c**hhhhhhhhhhhhhhh**c	88.24	0.75	+6
TsAP-S2	FLGMIPKLIKKLIKAFK c**hhhhhhhhhhhhhhh**c	88.24	0.73	+6

3.6. *Haemolytic effects of TsAPs*

The data obtained for each peptide in these assays are graphically represented in Fig. 8. TsAP1 was found to possess little haemolytic activity (6.48%) at the highest concentration tested (160 μM) (Fig. 8A). Compared with TsAP1, peptide TsAP2 demonstrated no haemolytic activity at concentrations up to and including 15 μM, but thereafter proved to be highly-haemolytic causing significant haemolysis at 40 μM (86%) and complete haemolysis at 80 μM and concentrations above (Fig. 8B). In contrast with their parent peptides, TsAP-S1 and TsAP-S2 caused significant haemolysis at 5 μM (28%) and complete haemolysis at concentrations of 20 μM and above (Fig. 8C and D).

3.7. *Anti-proliferative effects of TsAPs on human cancer cells*

The data obtained for each peptide in these assays are graphically represented in Fig. 9. TsAP-1 was only active in two of the five

Fig. 7. Helical wheel plots of TsAP-1, TsAP-S1, TsAP-2 and TsAP-S2. Note that both natural peptides have a hydrophobic face and a neutral face in contrast to both synthetic analogues in which the substitution of the neutral amino acid residues with positively-charged lysyl (K) residues has produced a classical amphipathic organisation with a hydrophobic face and a cationic face for microbial membrane interaction.

Table 3
Minimum inhibitory concentrations (MICs) and minimum bactericidal concentrations (MBCs) obtained using synthetic replicates of TsAP-1 and TsAP-2 and their enhanced cationicity analogues, TsAP-S1 and TsAP-S2, on the specified model test micro-organisms. NT – not tested.

Peptides	MIC (μM)			MBC (μM)		
	S. aureus	*E. coli*	*C. albicans*	*S. aureus*	*E. coli*	*C. albicans*
TsAP-1	120	160	160	>160	>160	>160
TsAP-2	5	>320	10	10	NT	10
TsAP-S1	2.5	5	2.5	20	20	5
TsAP-S2	5	5	2.5	20	40	10

human cancer cell lines tested and with HI57 and H838 cells, the IC_{50} values obtained were 55.9 μM and 52.5 μM, respectively (Fig. 9A and B). TsAP-2 was active against all five human cancer cell lines tested with IC_{50} values of 4.1 μM (H157), 11.0 μM (H838), 6.4 μM (MCF-7), 13.3 μM (PC3) and 15.4 μM (U251-MG) (Fig. 9A–E). In keeping with the antimicrobial activity data obtained for each analogue, significant increases in potency against all cancer cell lines were observed. TsAP-S1 was found to be active against all cancer cell lines tested with IC_{50} values of 1.5 μM (H157), 1.6 μM (H838), 1.8 μM (MCF-7), 2.1 μM (PC3) and 2.9 μM (U251-MG) (Fig. 9A–E). Thus the potency of TsAP-1 for H157 and H838 cancer cells was enhanced more than 30-fold by increasing its cationicity. TsAP-S2 also displayed increased potency against all five cell lines with IC_{50} values of 0.83 μM (H157), 1.6 μM (H838), 1.8 μM (MCF-7), 1.6 μM (PC3) and 2.0 μM (U251-MG) (Fig. 9A–E). Thus the potency of TsAP-2 for all the cancer cell lines was likewise increased by cationicity enhancement but was less than that observed for TsAP-1 being between 3.5 and 8.5-fold.

4. Discussion

Animal venoms still remain a largely-unexplored resource for the discovery of novel biologically-active molecules [1–4]. Among these animal venoms, those of scorpions possibly represent the most unexplored with probably less than 1% of the total number of known species having been studied in any detail [16]. Used predominantly in prey capture and in defence, these complex cocktails of unique molecules have been an important factor in the survival of scorpions for over 400 million years – a rare attribute in the natural world [1–4]. Scorpion venom has been used in traditional Chinese medicine for many centuries [17], and the specificity and potency of many component molecules has led to such being regarded as suitable candidates for either drug design or more commonly in target identification for such [18].

Scorpion venoms are composed of in excess of one hundred different components ranging from enzymes, peptides, nucleotides, lipids, mucoproteins, biogenic amines, phospholipases, hyaluronidases, α-helical antimicrobial peptides and other as yet uncharacterised substances [1–4]. Neurotoxins in scorpion venoms have evolved for the purposes of immobilising and/or killing also as a very effective defence against predators or con-specific rivals [1–4]. Other components, such as the phospholipases and hyaluronidases, in common with their established roles in many other types of venoms, can facilitate the spread of other more debilitating toxic components, thus enhancing the venom's destructive effects. More recently-discovered molecules, such as the α-helical antimicrobial peptides, may constitute an element of innate immune defence against invasion by pathogens [10,11].

In this study, two linear α-helical peptides have been identified in the venom of the Brazilian yellow scorpion, *Tityus serrulatus*. Initially predicted from "shotgun" cloned venom-derived cDNA that encoded their respective biosynthetic precursors, the mature peptides were subsequently located in and structurally-characterised from, reverse phase HPLC fractions of venom. The peptides were named TsAP-1 and TsAP-2 (***T****ityus* ***s****errulatus* **A**nti-microbial **P**eptide) and although both possessed antimicrobial activity, this was unremarkable for TsAP-1. TsAP-2 was effective against *S. aureus* (MIC 5 μM) and *C. albicans* (MIC 10 μM) but was ineffective against *E. coli* at even the highest concentration tested (320 μM). This was despite the fact that both peptides were very similar in primary structure, had the same number of amino acid residues (17) and had the same net positive charge at pH 7 (+2). However, secondary structure prediction analysis indicated that TsAP-2 had a higher helical content (76.47%) and hydrophobic moment (0.51 μH) than TsAP-1 (58.82% helix, hydrophobic moment 0.43 μH) – factors that may explain the observed discrepancy in antimicrobial activity. Analogues of each peptide with enhanced

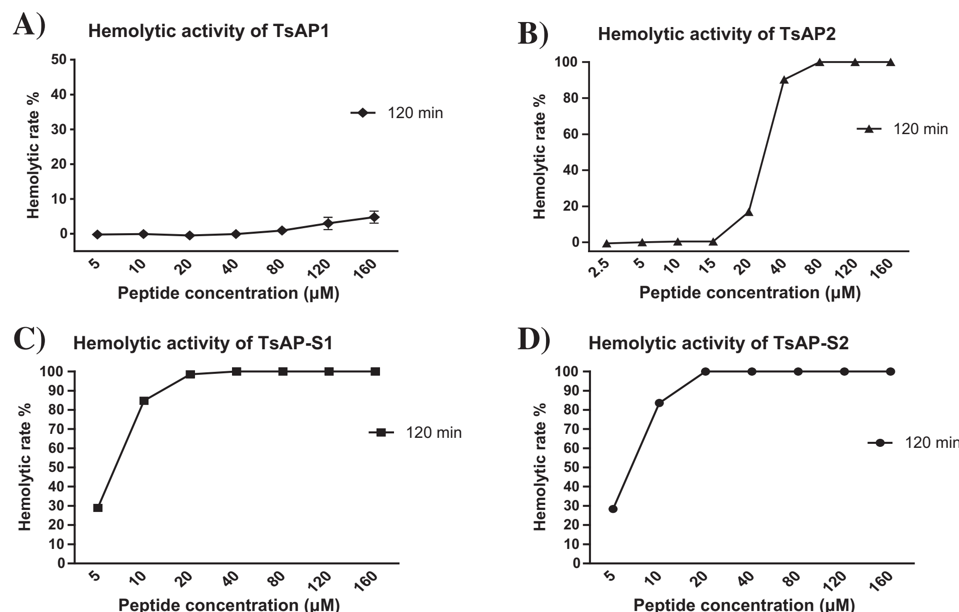

Fig. 8. Haemolytic activities of (A) TsAP-1, (B) TsAP-2, (C) TsAP-S1 and (D) TsAP-S2, following incubation with horse erythrocytes for 120 min.

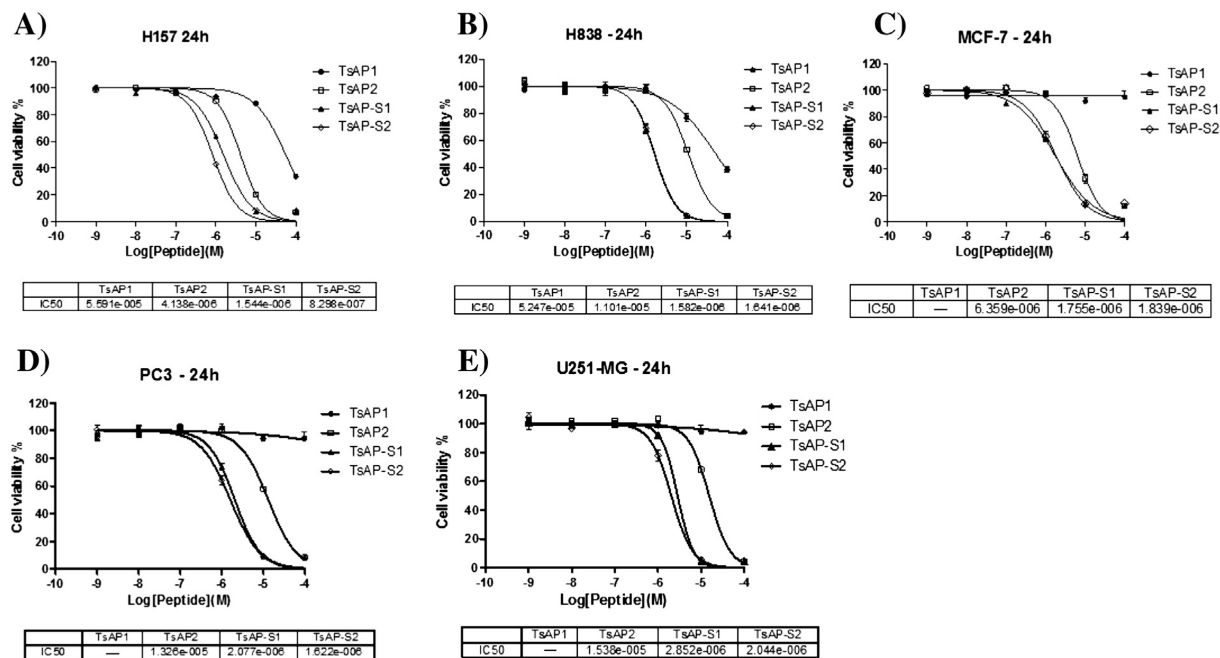

A)

	TsAP1	TsAP2	TsAP-S1	TsAP-S2
IC50	5.591e-005	4.138e-006	1.544e-006	8.298e-007

B)

	TsAP1	TsAP2	TsAP-S1	TsAP-S2
IC50	5.247e-005	1.101e-005	1.582e-006	1.641e-006

C)

	TsAP1	TsAP2	TsAP-S1	TsAP-S2
IC50	—	6.359e-006	1.755e-006	1.839e-006

D)

	TsAP1	TsAP2	TsAP-S1	TsAP-S2
IC50	—	1.326e-005	2.077e-006	1.622e-006

E)

	TsAP1	TsAP2	TsAP-S1	TsAP-S2
IC50	—	1.538e-005	2.852e-006	2.044e-006

Fig. 9. Anti-proliferative effects of TsAPs and their enhanced cationicity analogues on a panel of human cancer cell lines after 24 h incubation. Panels A–E illustrate their effects on H157 (squamous carcinoma lung), H838 (adenocarcinoma lung), MCF-7 (breast carcinoma), PC3 (prostate carcinoma) and U251-MG (glioblastoma) cancer cells, respectively. IC_{50} values are given for each peptide in panels below graphs.

cationicity (TsAP-S1 and TsAP-S2) were engineered by replacing strategically-placed residues with neutral side-chains by lysyl residues with positively-charged side-chains thus changing the net positive charge of each peptide to +6. An added benefit of these structural modifications was to increase the helical content of both peptides to 88.24% and the hydrophobic moments to 0.75 μH and 0.73 μH, respectively. These modifications produced significant effects on antimicrobial activity that were most pronounced for TsAP-1. TsAP-S1 displayed enhanced potency against all test organisms with a 48-fold increase in potency against *S. aureus*, a 32-fold increase in potency against *E. coli* and a 64-fold increase in potency against *C. albicans*. TsAP-S2, in contrast, remained equipotent against *S. aureus*, increased in potency 4-fold against *C. albicans* but increased in potency 64-fold against *E. coli*. In general terms, increasing the cationicity of an antimicrobial peptide enhances its antimicrobial effects and this assertion was effectively substantiated by the data presented in this study [19]. However, the situation is obviously more complex than this. The comparison of potencies between TsAP-1 and TsAP-2 would fully substantiate this effect but the comparison between TsAP-2 and TsAP-S2 was less clear. Here, the enhancement in potency against *E. coli* was most pronounced but was either negligible or minimal against *S. aureus* and *C. albicans*, respectively. Thus, modification of this peptide has apparently altered spectrum of activity rather than potency *per se*. While increasing the net positive charge of an antimicrobial peptide is known to increase its general antimicrobial potency, increasing the amphipathic nature of a peptide, either through segregating the hydrophobic face or by increasing hydrophobic moment, often results in enhanced mammalian cytotoxicity. A consequence of the engineered increase in cationicity of both peptides was that both of these parameters were also enhanced as evidenced by helical wheel plots and the dramatic increase in haemolytic activity observed, particularly for TsAP-1 (Table 2 and Fig. 7) [19]. While this may at first appear to be a deleterious effect with respect to an antimicrobial endpoint, it actually resulted in enhanced anti-cancer cell activity (Fig. 9). Of particular interest here was the fact that the majority of IC_{50} values for both peptide analogues against the majority of the human cancer cell lines tested, were below the concentrations that produced significant haemolysis. These data might imply that a more systematic study of the structural parameters that enable such peptides to apparently specifically affect the membranes of cancer cells rather than normal cells, may prove fruitful in the development of effective anti-cancer agents that could be used for systemic administration.

An interesting finding in the present study that resulted from bioinformatic analysis of peptide primary structural data, was that TsAP-1 exhibited significant structural identity to the phylloseptins – a family of antimicrobial peptides from South/Central American phyllomedusine frog skin Ref. [13] and that TsAP-2, exhibited the same degree of structural identity with the medusins – a most recently-described and novel family of skin peptides from the same source [14] (Figs. 3 and 4). This may be an example of convergent evolution dictated by natural selection for purpose rather than indicative of any phylogenetic relationship. Another example of this phenomenon that is well-documented is the occurrence of identical bradykinin structures from sources as diverse as mammals, amphibians and insects [20].

References

[1] R.C. Rodriguez de la Vega, E.F. Schwartz, L.D. Possani, Mining of scorpion venom biodiversity, Toxicon 56 (2010) 1155–1161.

[2] M.S. Bonnet, Toxicology of *Androctonus* scorpions, Br. Homoeopath. J. 86 (1997) 142–151.

[3] M. Goyffon, C. Landon, Scorpion toxins and defensins, C R Seances Soc. Biol. Fil 192 (1998) 445–462.

[4] E. Zlotkin, M. Eitan, V.P. Bindokas, M.E. Adams, M. Moyer, W. .Burkhart, E. Fowler, Functional duality and structural uniqueness of depressant insect-selective neurotoxins, Biochemistry 30 (1991) 4814–4821.

[5] A. .Keramidas, A.J. .Moorhouse, P.R. Schofield, P.H. Barry, Ligand-gated ion channels: mechanisms underlying ion selectivity, Prog. Biophys. Mol. Biol. 86 (2004) 161–204.

[6] L.D. Possani, E. Merino, M. Corona, F. Bolivar, B. Becerril, Peptides and genes coding for scorpion toxins that affect ion-channels, Biochimie 82 (2000) 861–868.

[7] M.L. Garcia, Y. Gao, O.B. McManus, G.J. Kaczorowski, Potassium channels: from scorpion venoms to high-resolution structure, Toxicon 39 (2001) 739–748.

[8] X.P. Zuo, Y.H. Ji, Molecular mechanism of scorpion neurotoxins acting on sodium channels: insight into their diverse selectivity, Mol. Neurobiol. 30 (2004) 265–278.
[9] P. Favreau, L. Menin, S. Michalet, F. Perret, O. Cheneval, M. Stöcklin, P. Bulet, R. Stöcklin, Mass spectrometry strategies for venom mapping and peptide sequencing from crude venoms: case applications with a single arthropod specimen, Toxicon 47 (2006) 676–687.
[10] D. Elgar, J.D. Plessis, L.D. Plessis, Cysteine-free peptides in scorpion venom: geographical distribution, structure-function relationship and mode of action, Afr. J. Biotechnol. 5 (2006) 2495–2502.
[11] X. Zeng, G. Corzo, R. Hahin, Scorpion venom peptides without disulfide bridges, IUBMB Life 57 (2005) 13–21.
[12] D.G. Nascimento, B. Rates, D.M. Santos, T. Verano-Braga, A. Barbosa-Silva, A.A. Dutra, I. Biondi, M.F. Martin-Eauclaire, M.E. De Lima, A.M. Pimenta, Moving pieces in a taxonomic puzzle: venom 2D-LC/MS and data clustering analyses to infer phylogenetic relationships in some scorpions from the *Buthidae* family (Scorpiones), Toxicon 47 (2006) 628–639.
[13] T. Chen, M. Zhou, R. Gagliardo, B. Walker, C. Shaw, Elements of the granular gland peptidome and transcriptome persist in air-dried skin of the South American orange-legged leaf frog, *Phyllomedusa hypochondrialis*, Peptides 27 (2006) 2129–2136.
[14] X. Xi, R. Li, Y. Jiang, Y. Lin, Y. Wu, M. Zhou, J. Xu, L. Wang, T. Chen, C. Shaw, Medusins: a new class of antimicrobial peptides from the skin secretions of phyllomedusine frogs, Biochimie 95 (2013) 1288–1296.
[15] A. Almaaytah, M. Zhou, L. Wang, T. Chen, B. Walker, C. Shaw, Antimicrobial/cytolytic peptides from the venom of the North African scorpion, *Androctonus amoreuxi*: biochemical and functional characterization of natural peptides and a single site-substituted analog, Peptides 35 (2012) 291–299.
[16] K.N. Srinivasan, P. Gopalakrishnakone, P.T. Tan, K.C. Chew, B. Cheng, R.M. Kini, J.L. Koh, S.H. Seah, V. Brusic, SCORPION, a molecular database of scorpion toxins, Toxicon 40 (2002) 23–31.
[17] C. Goudet, C.W. Chi, J. Tytgat, An overview of toxins and genes from the venom of the Asian scorpion *Buthus martensi* Karsch, Toxicon 40 (2002) 1239–1258.
[18] R.J. Lewis, M.L. Garcia, Therapeutic potential of venom peptides, Nat. Rev. Drug Discovery 2 (2003) 790–802.
[19] Y.S. Kim, H.J. Cha, Disperse distribution of cationic amino acids on hydrophilic surface of helical wheel enhances antimicrobial peptide activity, Biotechnol. Bioeng. 107 (2010) 216–223.
[20] J.M. Conlon, Bradykinin and its receptors in non-mammalian vertebrates, Regul. Pept. 79 (1999) 71–81.